Autonomous Robots 12, 157–172, 2002

Feedforward and Feedback Dynamic Trot Gait Control for Quadruped Walking Vehicle

RYO KURAZUME
The University of Tokyo, 4-6-1, Komaba, Meguro-ku, Tokyo 153-8505, Japan
kurazume@cvl.iis.u-tokyo.ac.jp

KAN YONEDA AND SHIGEO HIROSE
Tokyo Institute of Technology, 2-12-1, Oo-okayama Meguro-ku, Tokyo 152-8552, Japan
yoneda@mes.titech.ac.jp
hirose@mes.titech.ac.jp

Abstract. To realize dynamically stable walking for a quadruped walking robot, the combination of the trajectory planning of the body and leg position (feedforward control) and the adaptive control using sensory information (feedback control) is indispensable. In this paper, we propose a new body trajectory, the 3D sway compensation trajectory, for a stable trot gait; we show that this trajectory has a lower energy consumption than the conventional sway trajectory that we have proposed. Then, for the adaptive attitude control method during the 2-leg supporting phase, we consider four methods, that is, a) rotation of body along the diagonal line between supporting feet, b) translation of body along the perpendicular line between supporting feet, c) vertical swing motion of recovering legs, and d) horizontal swing motion of recovering legs; we then describe how we verify the stabilization efficiency of each method through computer simulation, stabilization experimentation, and experimenting in walking on rough terrain using the quadruped walking robot, TITAN-VIII.

Keywords: quadruped robot, trot gait, ZMP, energy efficiency, attitude control, swing legs control

1. Introduction

To increase the walking speed and the energy efficency of a quadruped walking vehicle, it is necessary to realize dynamically stable walking in cases where the vehicle body is supported by fewer than 3 legs and is therefore unstable.

In studying the trot (Yoneda and Hirose, 1995; Hirose et al., 1989; Yoneda et al., 1994, 1996), pace (Sano and Furusho, 1989), and bound (Raibert, 1986; Furusho et al., 1994, 1995) gaits, which are fundamental dynamically stable gaits, we have particularly noticed the trot gait because of its close affinity to the crawl gait, which is one of the standard statically stable gaits, and can be classified as a "safety gait" (Hirose and Yoneda, 1993) that avoids complete tumbling by touching a swing leg to ground. Consequently, in this paper we propose a generalized trot gait (Yoneda and Hirose, 1995; Hirose et al., 1989) which can smoothly shift from the crawl gait to the trot gait in proportion to walking speed, and an intermittent trot gait (Yoneda et al., 1996) which makes the diagonal legs swing and supports legs simultaneously to reduce the dynamic effect of the recovering swing legs on the body.

In addition we propose the sway compensation trajectory of the vehicle body (Yoneda and Hirose, 1995) which controls the position of a zero moment point (ZMP); we describe how we verify the effectiveness of this trajectory control to realize a dynamically stable walk by performing walking experiments using the TITAN-IV and TITAN-VI. ZMP is the projection onto the ground of the force acting on the body as shown in Fig. 1. At this point, no moment exists. Therefore, positioning this point on the diagonal line of the supporting

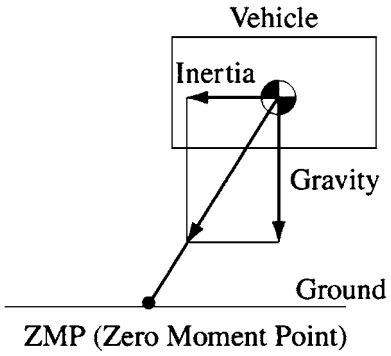

Figure 1. Zero moment point(ZMP).

legs while the robot is using the trot gait, enables the robot to keep walking stabley since there is no moment along this line which causes the inclination of the robot body. The proposed sway compensation trajectory uses lateral (along y axis) body motion to keep the ZMP on a diagonal line between the support legs as shown in Fig. 2.

The improvement of the energy efficiency for walking is one of the most important topics in design and control of a mobile vehicle. Especially, for mobile vehicles which have an energy source such as a battery, the improved energy efficiency realizes not only the extension of the work hours but also the increase of transportable weight by the miniaturization of the battery and concentrated utilization of limited resources for the desired task.

Kimura et al. (1990) examined the energy efficiency of a quadruped vehicle and showed the relation between the walking cycle and energy consumption for trot and pace gaits. However, a quadruped walking vehicle was modeled as an inverted pendulum and the dynamically stable gait which always maintains the equilibrium state, such as the gait realized by sway compensation trajectory, was not examined.

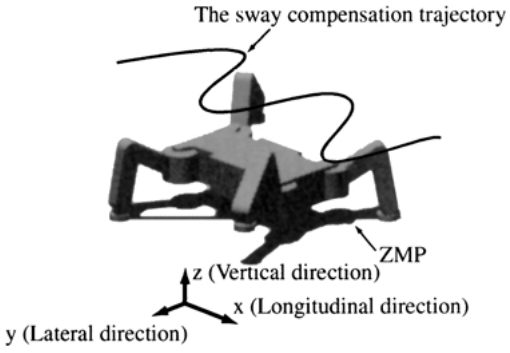

Figure 2. The sway compensation trajectory.

As design methodology, we also propos GDA (Gravitationally Decoupled Actuation) (Hirose and Yoneda, 1993; Hirose, 1984) which reduces energy consumption of the walking vehicle mechanically.

Then, if the sway compensation trajectory is examined from the viewpoint of energy efficiency, the energy consumption is expected to be larger than in the case without specific controls of body trajectory, since acceleration and deceleration of the body in the lateral direction along y axis has to be repeated periodically.

On the other hand, the position of ZMP is controllable not only by the lateral motion along the y axis but also by the longitudinal and vertical motion along the x and z axes, respectively. And thus, by combining these motions, it may be possible to improve the energy efficiency against the conventional sway compensation trajectory which controls the position of ZMP only by the lateral motion.

In this paper, we propose the 3D sway compensation trajectory of a vehicle body which uses lateral, longitudinal, and vertical motion of the vehicle body to move the ZMP on the diagonal line of the support legs. It is verified that the proposed trajectory improves the energy efficiency through theoretical analysis and the dynamic simulation software, ADAMS.

Furthermore, we point out that the body attitude becomes unstable and oscillates due to the dynamic effect of the recovering motion of the swing legs, when the generalized trot gait using the sway compensation trajectory in which the duty factor is 0.5–0.75 (Yoneda et al., 1996) is applied. In addition, though the 3D sway compensation trajectory can make dynamically stable walking on flat ground possible, stable walking is impossible by using only gait control planned by the 3D sway compensation trajectory when unknown roughness or inclination exists. Therefore, a feedback control system using mounted attitude sensors, gyroscope sensors, etc. which adaptively corrects the body attitude is required.

For the crawl gait, which is one of the standard statically stable gaits, several quadruped walking vehicles using attitude sensors (Hirose et al., 1984) or force sensors on the tip of the legs (Klein and Chung, 1987) to adapt to inclination of slope automatically have been developed. We also propose the "Sky-hook suspension control" (Yoneda et al., 1994) in which the specific impedance relation in the deviation from desired

position and attitude is established, and the body motion is controlled by force control using force sensors on the tip of the support legs. However, this method fundamentally owes the attitude stabilization control in statically stable walking gait in which 3 or more legs are in contact with the ground, and thus, stabilization performance for the two-leg supporting phase is not sufficient.

In contrast, Hiraki et al. (1996) previously proposed a method to produce the required moment for attitude recovery by rotating the body along the diagonal line between the support legs. In this method, the two-leg supporting phase is modeled as an inverted pendulum. But from the results of computer simulation examined later, the stabilization performance of this method is not always sufficient when the initial deviation of attitude is large.

In this paper, several attitude control methods, including body translation along the direction perpendicular to the diagonal line between the support legs, and the use of swing legs waving in the vertical and lateral direction to suppress the oscillation of attitude, are proposed. Then, we describe: how analytical models of each method are derived and optimum regulators are designed; and how the control performance of each method is compared through computer simulation and damping control experimentation in the two-leg supporting phase using the quadruped walking vehicle named TITAN-VIII (Arikawa and Hirose, 1996).

Furthermore, for the realization of the practical dynamically stable trot gait for a quadruped walking vehicle, we believe that the combination of feedforward control based on the sway compensation trajectory and feedback control based on the adaptive attitude control is one possible effective control method. The basic ideas underlying this feedforward and feedback dynamic trot gait control are as follows: first, the state of the system is generously transferred adjacent to the unstable equilibrium point by off-line, feedforward gait planning such as the sway compensation trajectory; then, the remaining small deviation from the equilibrium point is adaptively compensated for by a simple, linear feedback control system. In this paper, we describe how we developed the feedforward and feedback dynamic trot gait control system that combines the 3D sway compensation trajectory and the adaptive body position and swing leg motion control and the walking experiment on rough terrain using TITAN-VIII that was carried out.

2. 3D Sway Compensation Trajectory

2.1. Conventional Sway Compensation Trajectory

First, the formulation of the conventional sway compensation trajectory is shown. Here, we consider a vehicle as a point mass at (x_g, y_g, z_g). If the ground is flat and the height of the body from the ground, z, is constant, the position of ZMP $(x_z, y_z, 0)$ is given as

$$\begin{pmatrix} x_z \\ y_z \end{pmatrix} = \begin{pmatrix} x_g \\ y_g \end{pmatrix} - A \begin{pmatrix} \ddot{x}_g \\ \ddot{y}_g \end{pmatrix} \tag{1}$$

where, $A = \frac{z_g}{g}$. Next, the diagonal line of the support legs is defined as

$$\cos\theta\ x + \sin\theta\ y = d \tag{2}$$

Then, in order for ZMP to stay on this line, the center of gravity has to satisfy

$$\cos\theta(x_g - A\ddot{x}_g) + \sin\theta(y_g - A\ddot{y}_g) = d \tag{3}$$

Assuming that the vehicle moves along the x axis and acceleration of the center of gravity toward the moving direction is constant, the position of the body along the x axis is expressed as

$$x_g = a_2^x t^2 + a_1^x t + a_0^x \tag{4}$$

By substituting this equation into Eq. (3), we get

$$\begin{aligned} &\cos\theta\left(a_2^x t^2 + a_1^x t + a_0^x - 2Aa_2^x\right) \\ &\quad + \sin\theta(y_g - A\ddot{y}_g) = d \end{aligned} \tag{5}$$

The solution of this differential equation, y_g, is given as the addition of the solution of the next equation

$$y_g - A\ddot{y}_g = 0 \tag{6}$$

that is,

$$y_g = C_1^y e^{\frac{t}{\sqrt{A}}} + C_2^y e^{-\frac{t}{\sqrt{A}}} \tag{7}$$

and one particular solution that satisfies Eq. (5). Here, we assume that the general form of the particular solution is expressed by a polynominal expression of time t; then the solution of Eq. (5) is derived as

$$y_g = C_1^y e^{\frac{t}{\sqrt{A}}} + C_2^y e^{-\frac{t}{\sqrt{A}}} + a_2^y t^2 + a_1^y t + a_0^y \tag{8}$$

From the boundary condition about the continuity of trajectory ($\dot{y}_{g,t=0} = \dot{y}_{g,t=\frac{T}{2}} = 0,\ y_{g,t=0} = -y_{g,t=\frac{T}{2}}$), each coefficient is determined as

$$C_1^y = \sqrt{A}\cot\theta \frac{Ta_2^x + \left(1 - e^{-\frac{T}{2\sqrt{A}}}\right)v}{\left(e^{\frac{T}{2\sqrt{A}}} - e^{-\frac{T}{2\sqrt{A}}}\right)} \tag{9}$$

$$C_2^y = \sqrt{A}\cot\theta \frac{Ta_2^x + \left(1 - e^{\frac{T}{2\sqrt{A}}}\right)v}{\left(e^{\frac{T}{2\sqrt{A}}} - e^{-\frac{T}{2\sqrt{A}}}\right)} \tag{10}$$

$$a_2^y = -2a_2^x \cot\theta \tag{11}$$

$$a_1^y = -a_1^x \cot\theta \tag{12}$$

$$a_0^y = -a_0^x \cot\theta + d\csc\theta \tag{13}$$

$$a_0^x = \frac{d}{\cos\theta} + \frac{1}{2} \times \left(\frac{\sqrt{A}T\left(e^{\frac{T}{2\sqrt{A}}} + e^{-\frac{T}{2\sqrt{A}}} + 2\right)}{\left(e^{\frac{T}{2\sqrt{A}}} - e^{-\frac{T}{2\sqrt{A}}}\right)} - \frac{T^2}{4}\right) a_2^x - \frac{T}{4}a_1^x \tag{14}$$

Where, T is a walking cycle. This solution is a trajectory of the center of gravity that always keeps the ZMP on the diagonal line of the support legs, and this trajectory is defined as the (conventional) sway compensation trajectory.

2.2. *Expansion for Longitudinal Motion*

The conventional sway compensation trajectory mentioned above is expanded to the form including a sway toward the longitudinal direction.

First, Eq. (3) is decomposed into two equations for the x and y directions, and each solution trajectory is assumed to be given as Eq. (8) and

$$x_g = C_1^x e^{\frac{t}{\sqrt{A}}} + C_2^x e^{-\frac{t}{\sqrt{A}}} + a_2^x t^2 + a_1^x t + a_0^x \tag{15}$$

By substituting the boundary condition about the continuity of trajectory, the following equations with two parameters a_2^x and a_1^x are derived.

$$C_1^x = -\frac{(T^2 + 4\sqrt{A}T)a_2^x + 2Ta_1^x - 2L}{8\left(e^{\frac{T}{2\sqrt{A}}} - 1\right)} \tag{16}$$

$$C_2^x = -\frac{(T^2 - 4\sqrt{A}T)a_2^x + 2Ta_1^x - 2L}{8\left(e^{-\frac{T}{2\sqrt{A}}} - 1\right)} \tag{17}$$

$$C_1^y = \sqrt{A}\cot\theta \frac{Ta_2^x + \left(1 - e^{-\frac{T}{2\sqrt{A}}}\right)a_1^x}{\left(e^{\frac{T}{2\sqrt{A}}} - e^{-\frac{T}{2\sqrt{A}}}\right)} \tag{18}$$

$$C_2^y = \sqrt{A}\cot\theta \frac{Ta_2^x + \left(1 - e^{\frac{T}{2\sqrt{A}}}\right)a_1^x}{\left(e^{\frac{T}{2\sqrt{A}}} - e^{-\frac{T}{2\sqrt{A}}}\right)} \tag{19}$$

$$a_2^y = -a_2^x \cot\theta \tag{20}$$

$$a_1^y = -a_1^x \cot\theta \tag{21}$$

$$a_0^y = -a_0^x \cot\theta + d\csc\theta \tag{22}$$

$$a_0^x = \frac{d}{\cos\theta} + \frac{1}{2} \times \left(\frac{\sqrt{A}T\left(e^{\frac{T}{2\sqrt{A}}} + e^{-\frac{T}{2\sqrt{A}}} + 2\right)}{\left(e^{\frac{T}{2\sqrt{A}}} - e^{-\frac{T}{2\sqrt{A}}}\right)} - \frac{T^2}{4}\right) a_2^x - \frac{T}{4}a_1^x \tag{23}$$

Where, L is the body stroke in one walking cycle.

2.3. *Expansion for Vertical Motion*

Moreover, the above equations are expanded to the form including a sway in the vertical direction.

Considering $A = \frac{z_g}{g + \ddot{z}_g}$, the solution is assumed to be given as

$$z_g = C_1^z e^{\frac{t}{\sqrt{A}}} + C_2^z e^{-\frac{t}{\sqrt{A}}} + Ag \tag{24}$$

Where, A is an arbitrary constant. By substituting the boundary condition about the continuity of trajectory, coefficients with a parameter A are derived as

$$C_1^z = -\frac{Ag - H}{1 + e^{\frac{T}{2\sqrt{A}}}} \tag{25}$$

$$C_2^z = -\frac{(Ag - H)e^{\frac{T}{2\sqrt{A}}}}{1 + e^{\frac{T}{2\sqrt{A}}}} \tag{26}$$

Where, H is the body height at $t = 0, \frac{T}{2}$.

We define these expansions of conventional sway compensation trajectory toward longitudinal and vertical direction as "the 3D sway compensation trajectory". As stated above, after the fundamental trajectory parameters d, θ, and z_0 are determined, all 3D sway compensation trajectories that contain lateral and longitudinal movement can be expressed with only two parameters a_2^x and a_1^x, and if vertical movement is included, all trajectories are expressed with three parameters, a_2^x, a_1^x, and A.

2.4. *Energy Efficiency of the 3D Sway Compensation Trajectory*

The energy consumption of a walking vehicle is affected by many factors such as mass of the body and

legs, configuration of the degrees of freedom, trajectory of body and legs, the negative power at each actuator, etc. (Marhefka and Orin, 1997; Arikawa and Hirose, 1995). In this paper, however, the trajectory which minimizes the total of the external force applied dynamically, that is, the sum of squared acceleration through the entire trajectory as defined below, is considered.

$$\rho = \int_0^{\frac{T}{2}} \left(\ddot{x}_g^2 + \ddot{y}_g^2 + \ddot{z}_g^2\right) dt \tag{27}$$

Here, only a regular walk ($a_2^x = 0$) is considered for simplicity.

First, for the conventional sway compensation trajectory in which the body is moved only in a longitudinal direction, the sum of squared acceleration through the entire trajectory, ρ, is obtained by substituting $a_1^x = \frac{L}{T}$ into Eq. (27) as

$$\rho = \frac{L^2\left(\sqrt{A}\left(-1 + e^{\frac{T}{\sqrt{A}}}\right) - e^{\frac{T}{2\sqrt{A}}}\right)\cot^2\theta}{A\left(1 + e^{\frac{T}{2\sqrt{A}}}\right)^2 T^2} \tag{28}$$

Next, the proposed 3D sway compensation trajectory including a sway in the longitudinal direction is considered. Since the parameter that can be designed is a_1^x, a_1^x that minimizes sum of squared acceleration through the entire trajectory is given by solving

$$\frac{\partial \rho}{\partial a_1^x} = 0 \tag{29}$$

as

$$a_1^x = \frac{\left(1 + e^{\frac{T}{2\sqrt{A}}}\right)^2 LT}{\left(1 + e^{\frac{T}{2\sqrt{A}}}\right)^2 T^2 + 16A\left(-1 + e^{\frac{T}{2\sqrt{A}}}\right)^2 \cot^2\theta} \tag{30}$$

And the minimum of the sum of squared acceleration ρ is derived as

$$\rho = \frac{L^2\left(\sqrt{A}\left(-1 + e^{\frac{T}{\sqrt{A}}}\right) - e^{\frac{T}{2\sqrt{A}}}\right)\cot^2\theta}{A\left(\left(1 + e^{\frac{T}{2\sqrt{A}}}\right)^2 T^2 + 16A\left(-1 + e^{\frac{T}{2\sqrt{A}}}\right)^2 \cot^2\theta\right)} \tag{31}$$

By comparing Eqs. (28) and (31), the sum of the squared acceleration for the 3D sway compensation trajectory is smaller than the sum for the conventional sway compensation trajectory except $T = 0$, $\theta = \frac{\pi}{2}$, or $A = H/g = 0, \infty$.

Table 1. Minimum of squared acceleration.

	Lateral only	Lateral and longitudinal	Lateral, longitudinal, and vertical
ρ	0.623	0.334	0.331
(ρ_x)	0	0.155	0.153
(ρ_y)	0.623	0.179	0.175
(ρ_z)	0	0	0.003
a_1^x	0.2	0.107	0.107
A	0.0204	0.0204	0.0207

Next, for the 3D sway compensation trajectory including a sway in the vertical direction, even though two parameters a_1^x and A should be designed, deriving an analytical solution that minimizes the sum of the squared acceleration is impossible. Therefore, in the following simulation, the minimum of the sum of the squared acceleration is calculated repeatedly using the Newton method.

Simulation results for $T = 1$ [s], $H = 0.2$ [m], $L = 0.2$ [m], $\theta = 30$ [deg], and $d = 0$ are shown in Table 1. And Fig. 3 shows the obtained body trajectories for the conventional sway compensation trajectory, the expansion in the longitudinal direction, and the expansion in the longitudinal and vertical direction, respectively. In

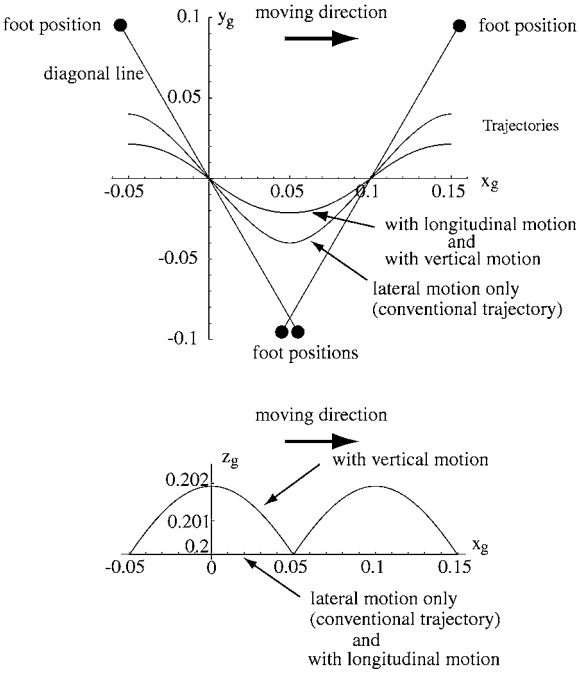

Figure 3. Trajectories of vehicle body.

Fig. 3, the upper figure shows the trajectories projected on the ground (x-y plane), and the lower figure shows the trajectories projected on the x-z plane from the lateral direction in which the vertical axis is magnified 20 times.

From these figures, it is verified that the sum of the squared acceleration can be reduced by swaying not only in the lateral direction but also in the longitudinal and vertical directions. This means that it might be possible to reduce energy consumption for walking.

Moreover, Figs. 4 and 5 show minimum of the sum of the squared acceleration for a change of θ which is the intersection angle between the y axis and diagonal line between the support legs, and the height of the body H, respectively. These figures show that the smaller the angle θ, that is, the diagonal line between the support legs lies perpendicularly to the moving direction, the more efficient the 3D sway compensation trajectory is.

Next, Fig. 6 shows the minimum of the sum of the squared acceleration for a change of walking cycle T. This figure shows that the effect of the 3D sway compensation trajectory increases as the walking cycle becomes shorter, and thus, walking speed increases.

And now, if the walking velocity $V = L/T$ is assumed to be constant in Eq. (31), we can derive that

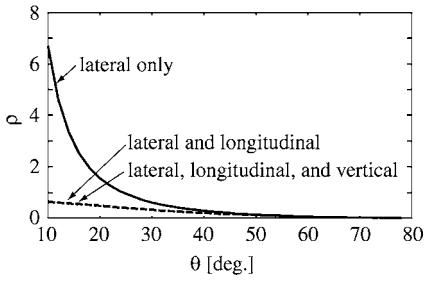

Figure 4. Effect of angle between the support legs ($T = 1$ [s], $H = 0.2$ [m], $L = 0.2$ [m], $d = 0$).

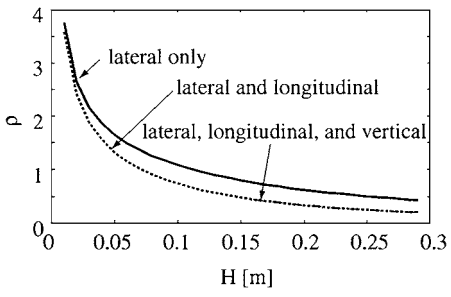

Figure 5. Effect of height of the body ($T = 1$ [s], $L = 0.2$ [m], $\theta = 30$ [deg.], $d = 0$).

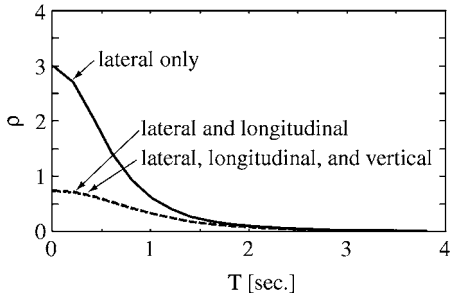

Figure 6. Effect of walking cycle ($H = 0.2$ [m], $L = 0.2$ [m], $\theta = 30$ [deg.], $d = 0$).

rho is monotone increasing, and $\rho = 0$ when $T \to 0$ and $\rho = \frac{V^2 \cot^2 \theta}{SqrtA}$ when $T \to \infty$. This means that for the purpose of reducing the sum of the squared acceleration ρ, the robot should walk with a very small walking cycle and a long slide.

Meanwhile, Kimura et al. (1990) proposed that there is a specific walking cycle which gives a minimum energy consumption when a robot walks by trot gait with a constant velocity. They adopted a model of an inverted pendulum as a modeling of the trot gait, and took an energy consumption due to the swing motion of legs into consideration. Therefore, in cases where the walking cycle is short, the energy consumption becomes large since swing legs have to be moved quickly. On the other hand, if the walking cycle is long, the body is inclined steeply, and thus, a large amount of energy is required to recover from the body inclination.

The maximization of energy efficiency, which includes the energy consumption of the leg motion or the energy dissipation due to the impact and friction between the feet and the ground, is very important and should be discussed. However, the energy efficiency depends on the leg structure, the design of an actuator and gear system, and the regeneration ratio of negative power produced at actuators. Therefore, as a more fundamental index, we adopted the sum of the squared acceleration during one walking cycle shown in Eq. (27) in this paper.

2.5. *Computer Simulation Using the Dynamic Motion Simulater, ADAMS*

To verify the energy efficiency of the 3D sway compensation trajectory that minimizes the sum of squared acceleration derived in Section 2.4, for the actual model with the same configuration of degrees of freedom as in a typical quadruped walking vehicle, the computer

simulation using the dynamic motion simulator, ADAMS,[1] was carried out. The simulation was executed on an Ultra sparc 30 Workstation of Sun Microsystems, Inc.

The configuration of degrees of freedom, weight, etc. of a quadruped walking vehicle model for computer simulation is the same as the TITAN-VIII (Arikawa and Hirose, 1996) which was developed in our laboratory.

Figures 7 and 8 show the computer model and an example of simulation results. The sum of power consumption at each joint and specific resistance ϵ (Gabrielli and Karman, 1950) are shown in Table 2 where the walking cycle is 1 [s], walking speed is 0.2 [m/s] and duty factor is 0.5. Specific resistance ϵ is the index term which makes unified evaluation of energy consumption possible even on a wall or horizontal surface.

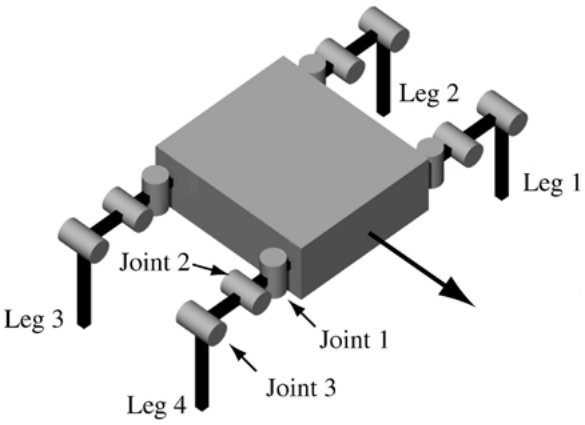

Figure 7. Simulation model for ADAMS.

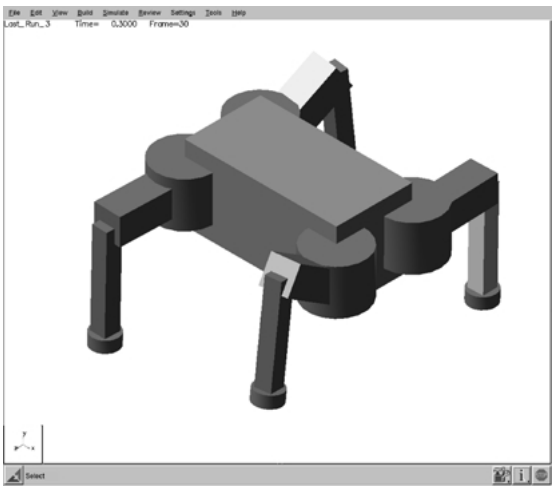

Figure 8. Simulation view of ADAMS.

Table 2. Comparison of energy consumption.

	Lateral only	Lateral and longitudinal	Lateral, longitudinal, and vertical	Straight
Energy cons. [J]	142.0	114.6	108.6	96.8
Specific res.	2.35	1.90	1.80	1.60

$$\epsilon \equiv \frac{(\textit{energy consumption of transfer})}{(\textit{vehicle weight}) \times (\textit{distance of movement})} \tag{32}$$

Specific resistance becomes smaller with higher transfer efficiency, and is minimized if the energy for the transfer is equal to the difference of potential energy before and after the transfer. That is to say, the highest value is 0 on a horizontal surface, and 1 on a vertical surface. The columns show the results of the conventional sway compensation trajectory, the trajectory including lateral and longitudinal sway, the trajectory including lateral, longitudinal, and vertical sway, and straight line with no sway control. The trajectories that minimize the sum of squared acceleration derived in Section 2.4 are used for the 3D sway compensation trajectories. In the case in which the body moves on a straight line with no sway control, however, the body attitude cannot be maintained to be parallel to the ground, and the swing leg touches the ground unexpectedly.

From these results, by using the 3D sway compensation trajectory that minimizes the sum of squared acceleration, specific resistance improves more than for conventional sway compensation trajectory even for the same walking cycle and walking speed.

And Fig. 9 shows power consumption at each joint of leg 2. In particular, power consumption at joint 3, which mainly produces the lateral sway motion, becomes low.

Next, we compare the power consumption between the conventional sway compensation trajectory and the 3D sway compensation trajectory for three models with different body lengths shown in Fig. 10. In this simulation, the walking cycle is 1 [s], walking speed is 0.2 [m/s] and duty factor is 0.5. The size of the model shown in Fig. 10(b) is the same as TITAN-VIII, and the models in Fig. 10(a) and (c) have half and double body length, respectively.

Table 3 shows the specific resistance and power consumption for these models. It is verified that the effect of the 3D sway compensation trajectory increases as

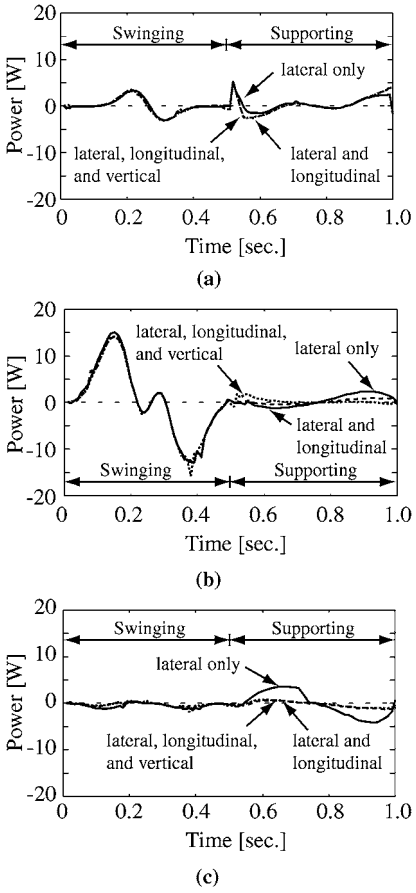

Figure 9. Power consumption of each joint of leg 2. (a) Joint 1; (b) Joint 2; (c) Joint 3.

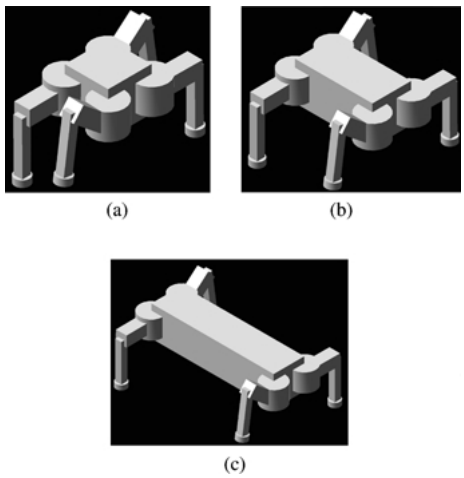

Figure 10. Three simulation models with different body length. (a) Short body length; (b) Middle body length; (c) Long body length.

Table 3. Specific resistance for each body length.

	(a) Lateral only	(b) 3D sway	(b)/(a)
Short	3.90 (236.0[J])	1.90 (114.5[J])	48.7 [%]
Middle	2.35 (142.0[J])	1.80 (108.6[J])	76.6 [%]
Long	1.81 (109.4[J])	1.75 (105.4[J])	96.7 [%]

the distance between the fore and hind legs shortens, and the angle of the diagonal line between the support legs in the moving direction becomes perpendicular.

3. Adaptive Attitude Control Methods

Even though the 3D sway compensation trajectory proposed above can realize dynamically stable walking on flat ground, stable walking is impossible using only gait control planned with the 3D sway compensation trajectory when unknown roughness or inclination exists. In addition, for example, when an extended trot gait with the sway compensation trajectory is applied, body attitude sometimes becomes unstable and oscillates due to the dynamic effect of the recovering motion of the swing legs, because the point mass is assumed for the derivation of the sway compensation trajectory (Yoneda et al., 1996).

Therefore, a feedback control system that uses mounted attitude sensors, gyroscope sensors, etc. which adaptively corrects body attitude is required. In this section, we propose the attitude control method during 2-leg supporting phase using the body translation and rotation, and leg swing motion.

To produce the required moment for attitude recovery in the two-leg supporting phase, the method using rotation of the body along the diagonal line between the support legs as shown in as shown in Fig. 11(a) has been proposed so far (Hiraki et al., 1996). The required moment for attitude recovery, however, can be produced by the translation of body position as shown in Fig. 11(b). Furthermore, although the recovery motion of swing legs has been considered as disturbance that induces the oscillation of body, so far (Yoneda et al., 1996), by controlling the recovery path appropriately, swing legs can be used for the oscillation control of body attitude.

From the above discussion, four stabilization control methods of body attitude as shown in Fig. 11 are considered in this paper.

(a) Rotation of the body along the diagonal line between the support legs.

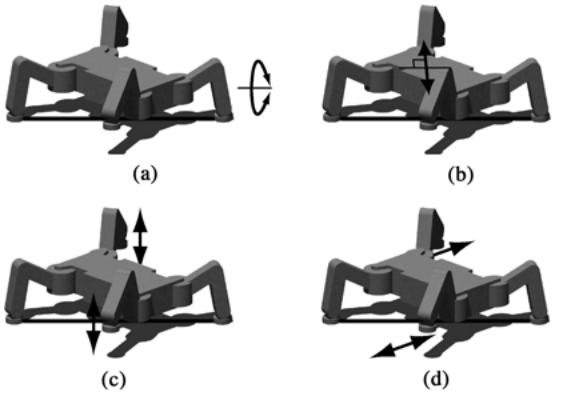

Figure 11. Four attitude control methods. (a) Rotation of body; (b) Translation of body; (c) Vertical motion of swing legs; (d) Horizontal motion of swing legs.

(b) Translation of the body along the direction perpendicular to the diagonal line between the support legs.
(c) Vertical motion of swing legs during recovery.
(d) Horizontal motion of the swing legs during recovery.

First, each method is simplified as a three-link model corresponding to a support leg, a body, and a swing leg as shown in Fig. 12. Appendix A shows motion equations of each model and derived optimum regulators designed to repress the oscillation of the body.

Fig. 13 shows examples of computer simulation when the initial conditions are $\phi_1 = 5$ [deg.], $\phi_2 = 0$ [deg.], and $x = 0$ [deg.]

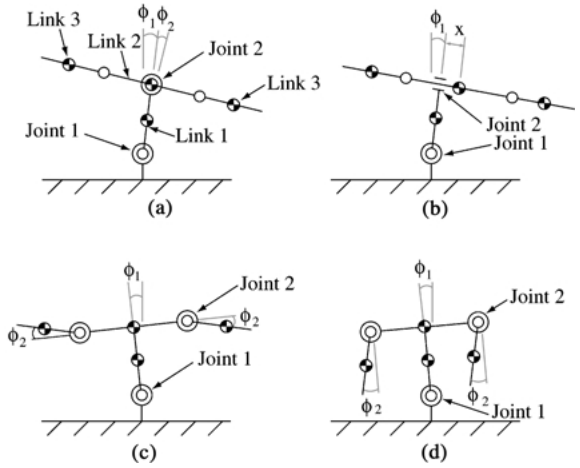

Figure 12. Analysis models. (a) Rotation of body; (b) Translation of body; (c) Vertical motion of swing legs; (d) Horizontal motion of swing legs.

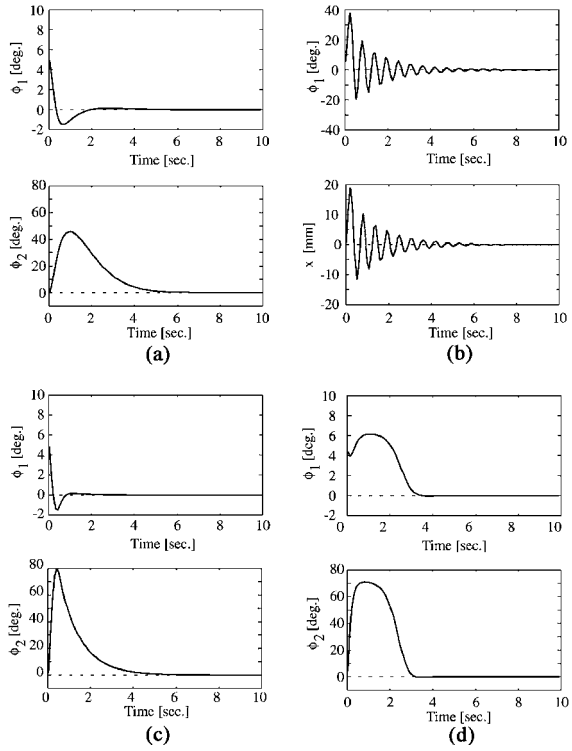

Figure 13. Simulation results. (a) Rotation of body; (b) Translation of body; (c) Vertical motion of swing legs; (d) Horizontal motion of swing legs.

From Fig. 13(a), the body has to be inclined up to 40 degrees toward the inclination direction to recover the inclination of the support leg for the method using the rotation of body. Figure 13(b) shows that maximum body movement to recover the inclination of the support leg is 0.2 [m] for the method using the translation of body. Though this body motion can be executed by TITAN-VIII, the inclination of the support leg becomes vibrational. Next, in Fig. 13(c) and (d), the maximum angles of the swing legs become 80 [deg.] and 70 [deg.], respectively. Thus, it is difficult to stabilize the body attitude using only the effect of vertical and horizontal motion of the swing legs since the realization of such a wide movable angle is difficult.

4. Dynamically Stable Walking Experiment with TITAN-VIII

4.1. Damping Control in the Two-Leg Supporting Phase

The damping control experiment using four attitude stabilization control methods examined in Section 3

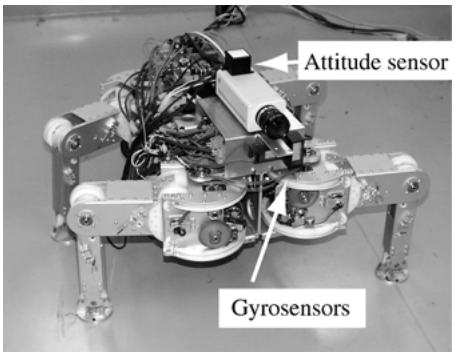

Figure 14. 4-legged walking robot, TITAN-VIII.

was carried out using the quadruped walking robot named TITAN-VIII.

As shown in Fig. 14, this robot is equipped with a computer board (Pentium 200 MHz, Japan Data System), AD/DA boards, Ethernet card, silicon disk, 3-axes attitude sensor, (Maxcube, Japan Aviation Electronics), and two gyrosensors (Gyrostar, Murata).

In the experiment, the body of TITAN-VIII that stood with two support legs was tilted by an external force applied to the body (pushing by hand), and the body attitude returned to the stable state by each control method was measured.

The ankle of TITAN-VIII is restricted mechanically to let the sole be parallel to the body. Thus, as shown in Fig. 15, the body attitude returns to a stable state without attitude control if the inclination angle is smaller than about 8 [deg.], since the moment for recovery of body inclination is produced by the soles.

For the purpose of increasing the dynamic effect of the swing legs to the body, the swing legs are stretched laterally in the middle of the return path as shown in Fig. 16(b), and therefore, the inertia of the legs is increased.

Inclination angle of the support leg along the diagonal line between the support legs, ϕ_1, and control variables ϕ_2 and x for each control method are shown

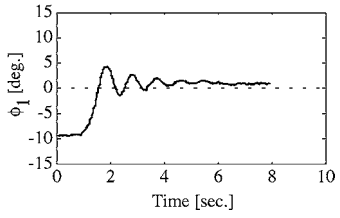

Figure 15. Experimental result (no sensor).

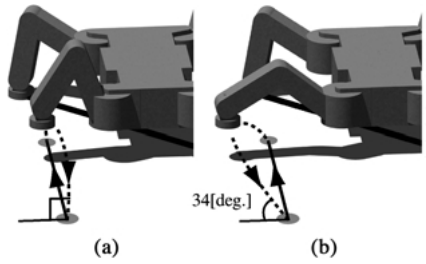

Figure 16. Recovering path of swing legs. (a) Recovering path is perpendicular to ground; (b) Recovering path is inclined with respect to ground.

in Fig. 17. Here, ϕ_2 in Fig. 17(a) is the body rotation angle, x in Fig. 17(b) is the body displacement, and ϕ_2 in Fig. 17(c) and (d) is the angle of joint 2 in Fig. 12 converted from the amount of swing.

Figure 18 shows the damping control experiment using the vertical motion of the swing legs, and where the swing legs are swung up as the recovery of body attitude. From the experimental results for the method

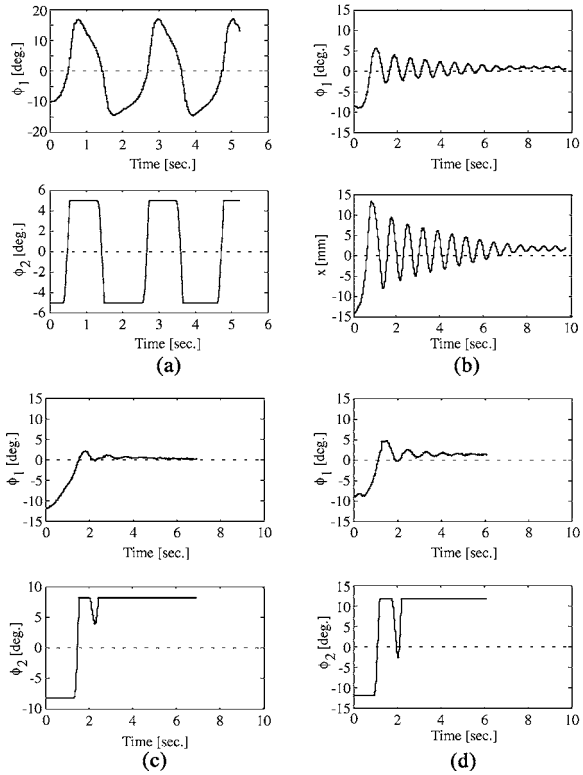

Figure 17. Experimental results of attitude control for slow trot gait. (a) Rotation of body; (b) Translation of body; (c) Vertical motion of swing legs; (d) Horizontal motion of swing legs.

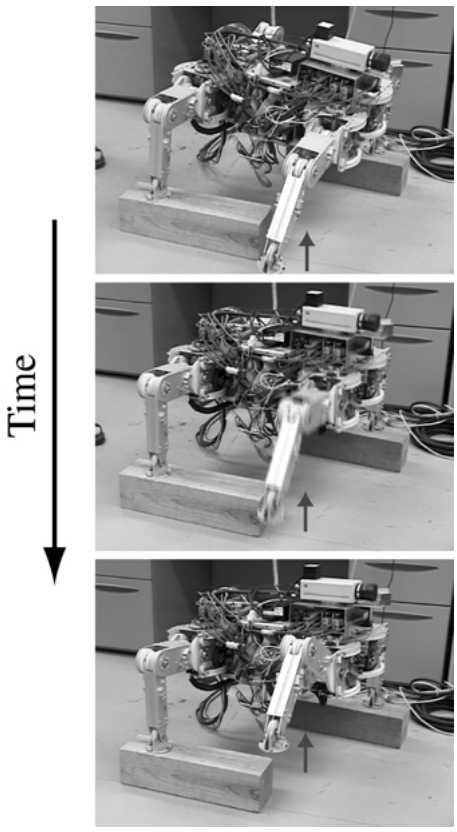

Figure 18. Experiment of attitude control using swing legs.

using the rotation of body shown in Fig. 17(a), the swing leg of the leaning side contacted the ground because the body was tilted more and more in the tilted direction, and large body vibration was generated by the reaction force. Next, for the method using the translation of the body shown in Fig. 17(a), though the body attitude was vibrational, it was finally converged to horizontal. From the comparison of Fig. 17(c) and Fig. 15 which are the results for the control method using vertical motion of the swing legs and the results without attitude control, performance of convergence was clearly improved by the dynamic effect of swinging. However, the swing width of the swing leg is limited in the joint movable area, and thus, recovery from a large tilt angle to horizontal is difficult using only this method. On the other hand, Fig. 17(d) using the horizontal motion of the swing legs shows the convergence performance is hardly improved since displacement of actual links is smaller than the case using vertical motion of the swing legs, and the dynamic effect is small.

These results suggest that the attitude stabilization performance might be the highest by combining the vertical motion of the swing legs and translation of the body.

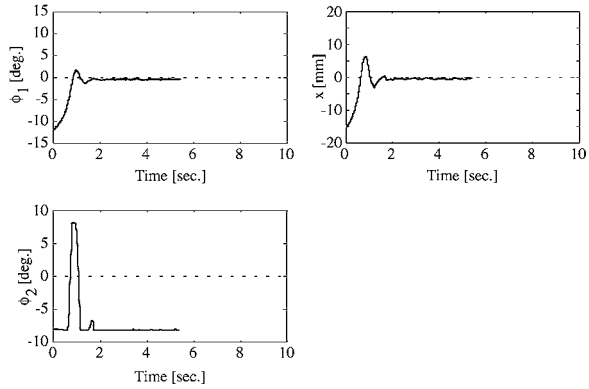

Figure 19. Experimental result (Combination of translation of body and vertical motion of swing legs).

Then, Fig. 19 shows the experimental result when these two methods are simply superimposed. In comparison with Fig. 19, Fig. 15 and Fig. 17(b), both convergence performance and stability are improved.

In general, the crawl gait, which is one of the statically stable walking gaits for a quadruped walking vehicle, makes it possible to walk maintaining static stability of the body, since three or more legs always have contact with the ground. However, in order to keep the projected point of the center of gravity within the support leg polygon, and also to guarantee the convergence to the regular gait, the possible area for the swing leg to contact the ground is limited compared with the movable area of leg. On the other hand, the possible area of the contact point for the trot gait can be taken wider than the crawl gait, since two diagonal legs turn into swing legs simultaneously. Therefore, if a stable trot gait can be realized using the proposed stabilization control even at low walking speed, the more adaptive walking with a large contact area will become possible.

4.2. Attitude Control Experiment by Generalized Trot Gait and Step Climbing Experiment

The attitude stabilization method which employs feedback control using vertical motion of the swing legs and translation of body, and feed forward control using the 3D sway compensation trajectory proposed in Section 2 was applied to TITAN-VIII, and the stabilization performance in dynamically stable walking by a generalized trot gait was verified.

As stated above, body attitude sometimes becomes vibrational when the duty factor is 0.5–0.75 for the generalized trot gait with the sway compensation trajectory by the dynamic effect of recovering motion of swing legs.

The body attitude of TITAN-VIII using the proposed body attitude stabilization control was then examined. Figure 20 shows a comparison with and without the attitude control, and Fig. 21 shows the measured inclination angle of the support legs around the diagonal line between the support legs. In this experiment, the duty factor is 0.65, walking cycle is 3 [s] and walking speed is 0.65 [m/s].

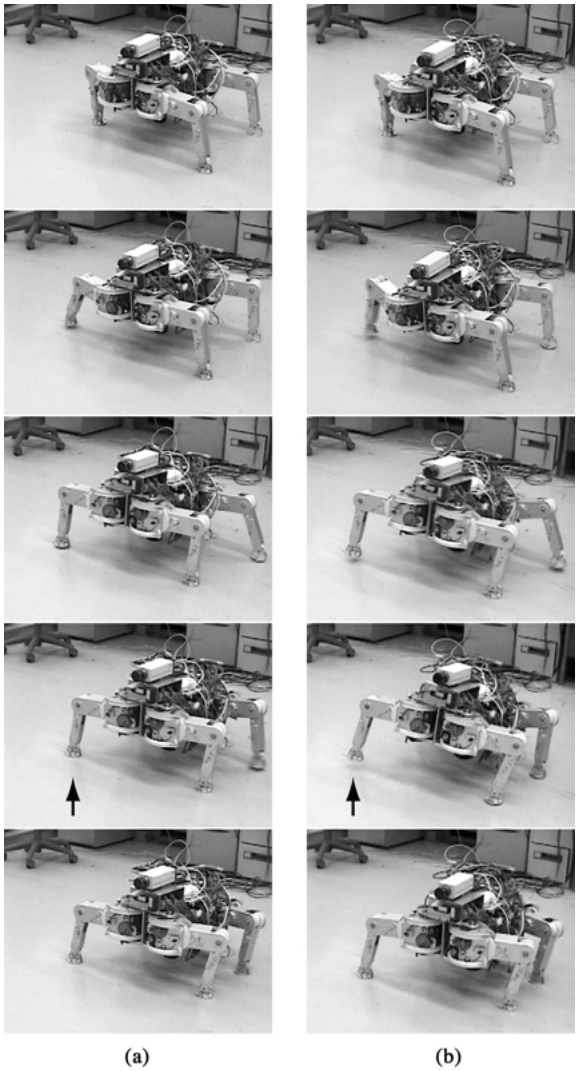

Figure 20. Dynamically stable walking experiment (Duty factor is 0.65). (a) attitude control; (b) no sensor.

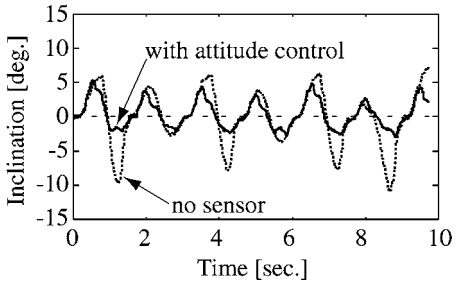

Figure 21. Body inclination (Duty factor is 0.65).

From Fig. 20, the inclination angle without attitude control was greatly collapsed as shown in the 3rd and 4th photos from the top. However, by the proposed attitude control, the right and left legs turned into swing legs equally. Accordingly, dynamically stable walking using a generalized trot gait with a duty factor of 0.65 can be realized by proposed body attitude stabilization control.

In addition, the return path of the swing legs is also shown in Fig. 22. The horizontal axis is the walking direction, and the vertical axis is the vertical direction. By using swing leg control only in the region where the height of the swing leg from the ground is larger than a specific height (5 [cm]), the body vibration caused by the contact of the swing leg to the ground is prevented.

Next, we examined the attitude stabilization performance when TITAN-VIII walks dynamically in an environment where an unknown and leaning step exists.

Figure 23 is a series of photos of the experiment, and Fig. 24 shows the inclination angle of the support leg around the diagonal line between the support legs. In this experiment, the duty factor is 0.5, walking cycle is 10 [s], and walking velocity is 0.02 [m/s]. The photos on the left in Fig. 23 show the results with the proposed attitude stabilization control, and the photos on the right show the results without attitude stabilization control.

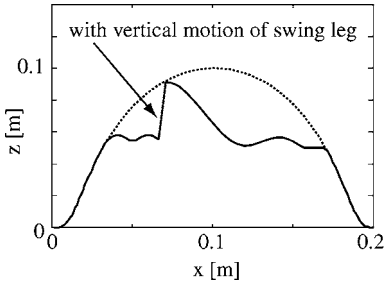

Figure 22. Recovering path of swing leg.

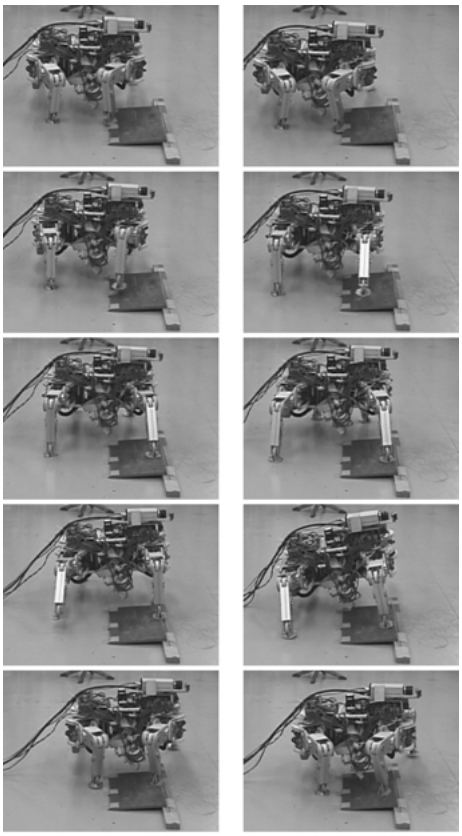

Figure 23. Dynamically stable walking experiment on rough terrain. (a) attitude control; (b) no sensor.

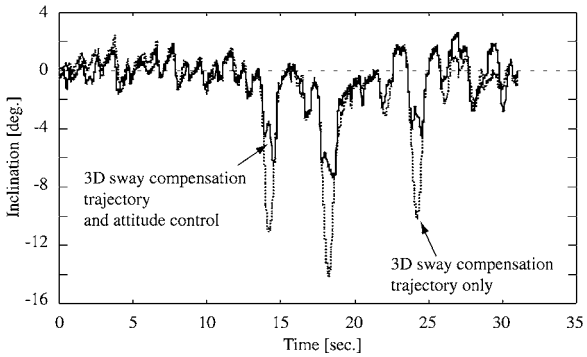

Figure 24. Body inclination of robot walking dynamically on rough terrain.

From Fig. 24, dynamically stable walking with small attitude fluctuation can be performed by the 3D sway compensation trajectory on a flat surface in 0–12 [s], On the other hand, one of the right side legs runs on the step in 12–25 [s]. The results without attitude control show that the body inclined so much and the swing leg contacted the ground unexpectedly as shown in the fourth photo of Fig. 23. However, when the proposed attitude stabilization control was applied, dynamically stable walking without contact of the swing legs to the ground was realized and the effectiveness of the proposed attitude stabilization control was confirmed.

5. Conclusion

In this paper, the 3D sway compensation trajectory, that is, an expansion of the conventional sway compensation trajectory with lateral motion toward the 3D trajectory including longitudinal and vertical motion, is proposed. The 3D sway compensation trajectory enables keeping ZMP on the diagonal line of the support legs more efficiently with less energy consumption. Then, it is verified that the proposed trajectory improves the specific resistance through theoretical analysis and the dynamic simulation software, ADAMS. The effect of the proposed trajectory increases as the vehicle walks faster, and even for the same walking speed, the proposed trajectory is especially effective when the movable range of the body is mechanically restricted since the swing length becomes smaller than when using the conventional sway compensation trajectory.

As stated above, the energy consumption of a walking vehicle is affected by many factors. The trajectory proposed in Section 2.4 that minimizes the sum of the squared acceleration, does not always consist of the optimum trajectory that minimizes the actual energy consumption for walking. For example, if the leg of a walking vehicle shown in Fig. 7 lies on a straight line, the required joint torque to support the force toward this direction is very small and walking with little energy consumption becomes possible using this straight form continuously.

On the other hand, for the proposed 3D sway compensation trajectory, all trajectories can be described with two or three parameters. Therefore, it might be possible to obtain the optimum trajectory that minimizes the energy consumption for an actual walking vehicle with various joint configuration, by repeat calculation with ADAMS, and this will be examined in the future.

Moreover, even though the 3D sway compensation trajectory proposed in this paper can realize dynamically stable walking on flat ground, stable walking is impossible using gait control planned with the 3D sway compensation trajectory only when unknown

roughness or inclination exists. In addition, for example, when an extended trot gait with the sway compensation trajectory is applied, body attitude sometimes becomes unstable and oscillates due to the dynamic effect of the recovering motion of the swing legs, because the point mass is assumed for the derivation of the sway compensation trajectory (Yoneda et al., 1996).

For these problems, in this paper, several attitude control methods including body translation along the direction perpendicular to the diagonal line between the support legs and the use of swing legs waving in the vertical and lateral direction to suppress the oscillation of attitude, are proposed to realize dynamically stable walking for the quadruped walking vehicle.

Then, the analytical model of each method was derived and the optimum regulator to stabilize the attitude oscillation was designed. The control performance of each method was compared through computer simulation and damping control experiment using the quadruped walking vehicle, TITAN-VIII, standing with two support legs.

Furthermore, a dynamically stable walking experiment on rough terrain using the generalized trot gait employing the 3D sway compensation trajectory and the proposed attitude control method was carried out, and the effectiveness of the proposed attitude control method that enables dynamically stable walking on unknown and rough terrain was confirmed.

So far, we have considered that a light weight leg is a requisite for the development of a practical walking vehicle and created them by the optimization of actuator configuration using, for example, wire and pulley, the use of light and rigid materials, and optimum mechanical design with high stiffness-weight ratio. However, experimental results show that even the light weight leg such as the leg of TITAN-VIII is effective for vibration control of the body depending on the moving direction.

The basic idea underlying the attitude stabilization control method proposed in this paper is as follows: First, the state of the system is generously transferred adjacent to the unstable equilibrium point by off-line gait planning using the 3D sway compensation trajectory. Then, the little deviation from the equilibrium point is adaptively compensated for by a simple linear feedback control system which utilizes the translation of the body and swinging of the swing legs.

Results of the experiment demonstrated that this control methodology was very effective for practical use and could make dynamically stable walking of walking vehicle possible.

Appendix A: Motion Equations for Three Link Models and Design of Optimum Regulators

A.1. Vibration Control Using Rotation of Body Along the Diagonal Line Between Support Legs

In Fig. 12(a), we assume that each link length, mass, and inertial are $l_i, m_i, I_i (i = 1\text{–}3)$, respectively. The motion equation of this model is derived as

$$\ddot{\phi}_1 = -\frac{M - \frac{gl_1(m_1+2m_2+4m_3)}{2}\phi_1}{I_1 + \frac{m_1+4m_2+8m_3}{4}l_1^2} \tag{33}$$

$$\ddot{\phi}_2 = \frac{M - \left(I_2 + 2I_3 + 2m_3\left(\frac{l_2+l_3}{2}\right)^2\right)\ddot{\phi}_1}{I_2 + 2I_3 + 2m_3\left(\frac{l_2+l_3}{2}\right)^2} \tag{34}$$

By substituting the parameters of TITAN-VIII into the above equations, and if the maximum torque is 10 [Nm], the optimum regulator is designed as

$$M = 118.0\phi_1 + 20.0\dot{\phi}_1 + 1.0\phi_2 + 1.87\dot{\phi}_2 \tag{35}$$

A.2. Vibration Control Using Translation of Body Along the Direction Perpendicular to the Diagonal Line Between the Support Legs

The motion equation of the model shown in Fig. 12(b) is derived as

$$\ddot{\phi} = \frac{m_1 g\frac{l_1}{2}\phi - m_2 g x + l_1 F}{I_1 + I_2 + \frac{1}{4}m_1 l_1^2} \tag{36}$$

$$\begin{aligned}\ddot{x} = &\left(\frac{m_1 g\frac{l^2}{2}}{I_1 + I_2 + \frac{1}{4}m_1 l_1^2} - g\right)\phi \\ &- \left(\frac{m_2 gl}{I_1 + I_2 + \frac{1}{4}m_1 l_1^2} - g\right)x \\ &+ \left(\frac{l^2}{I_1 + I_2 + \frac{1}{4}m_1 l_1^2} + \frac{1}{m}\right)F\end{aligned} \tag{37}$$

By substituting the parameters of TITAN-VIII into the above equations, and if the maximum force is 100 [N], the optimum regulator is designed as

$$F = 1543.8\phi + 275.7\dot{\phi} - 5006.5x - 883.3\dot{x} \tag{38}$$

A.3. Vibration Control Using Vertical Motion of the Swing Legs During Recovery

The motion equation of the model shown in Fig. 12(c) is derived as

$$\ddot{\phi}_1 = -\frac{2M - \frac{gl_1(m_1+2m_2+4m_3)}{2}\phi_1}{I_1 + I_2 + \frac{m_1+4m_2+8m_3}{4}l^2 + \frac{m_3 l_2^2}{2}} \tag{39}$$

$$\ddot{\phi}_2 = \frac{M - \left(I_3 + m_3\frac{l_3^2}{4} + m_3 l_2 \frac{l_3}{2}\cos\phi_2\right)\ddot{\phi}_1}{I_3 + m_3\frac{l_3^2}{4} + \frac{m_3 l_2 l_3}{4}\cos\phi_2} \tag{40}$$

By substituting the parameters of TITAN-VIII into the above equations, and if the maximum torque is 10 [Nm], the optimum regulator is designed as

$$M = 140.9\phi_1 + 27.6\dot{\phi}_1 + 1.0\phi_2 + 1.49\dot{\phi}_2 \tag{41}$$

A.4. Vibration Control Using Horizontal Motion of the Swing Legs During Recovery

The motion equation of the model shown in Fig. 12(d) is derived as

$$\ddot{\phi}_1 = -\frac{2M - \frac{gl_1(m_1+2m_2+4m_3)}{2}\phi_1}{I_1 + I_2 + \frac{m_1+4m_2+8m_3}{4}l_1^2 + \frac{m_3 l_2^2}{2}} \tag{42}$$

$$\ddot{\phi}_2 = \frac{M - gm_3\frac{l_3}{2}\sin(\phi_1+\phi_2)}{I_3 + m_3\frac{l_3}{2}^2 - m_3 l_1 \frac{l_3}{2}\cos\phi_2} - \frac{\left(I_3 + m_3\frac{l_3^2}{4} - m_3 l_1 l_3 \cos\phi_2\right)\ddot{\phi}_1}{I_3 + m_3\frac{l_3 r}{4} - m_3 l_1 \frac{l_3}{2}\cos\phi_2} \tag{43}$$

By substituting the parameters of TITAN-VIII into the above equations, and if the maximum torque is 10 [Nm], the optimum regulator is designed as

$$M = 122.7\phi_1 + 22.2\dot{\phi}_1 - 8.9\phi_2 - 0.56\dot{\phi}_2 \tag{44}$$

Note

1. Mechanical Dynamics, Inc., Ann Arbor, Michigan, USA.

References

Arikawa, K. and Hirose, S. 1995. Study of walking robot for 3 dimensional terrain. In *Proc. of IEEE/RSJ Int. Conf. on Intelligent Robots and Systems '95*, pp. 703–708.

Arikawa, K. and Hirose, S. 1996. Development of quadruped walking robot TITAN-VIII. In *Proc. of IEEE/RSJ Int. Conf. on Intelligent Robots and Systems '96*, pp. 208–214.

Furusho, J., Sano, A., Sakaguchi, M., and Honda, K. 1994. Bounce gait control of a quadruped robot. In *Proc. of the Second International Conference on Motion and Vibration Control*, vol. 1, pp. 198–203.

Furusho, J., Sano, A., Sakaguchi, M., and Koizumi, E. 1995. Realization of bounce gait in a quadruped robot with articlar-joint-type legs. In *Proc. Int. Conf. on Robotics and Automation*, pp. 697–702.

Gabrielli, G. and von Karman, I. 1950. What price speed? *Mechanical Engineering*, 72(10):775–781.

Hiraki, M., Emura, T., Senta, Y., and Okada, S. 1996. Trotting gait of a quadruped robot based on reaction wheel model (in Japanese). In *Proc. of 14th Conference of the Robotics Society of Japan*, pp. 967–968.

Hirose, S. 1984. A study of design and control of a quadruped walking vehicle. In *Int. J. Robotics Research*, 3(2):113–133.

Hirose, S., Nose, M., Kikuchi, H., and Umetani, Y. 1984. Adaptive gait control of a quadruped walking vehicle. *Robotics Research (1st Int. Symp.)*, Cambridge, MA: The MIT Press, pp. 253–277.

Hirose, S. and Yoneda, K. 1993. Toward the development of practical quadrupe walking vehicles. *J. of Robotics and Mechatronics*, 5(6):498–504.

Hirose, S., Yoneda, K., Furuya, R., and Takagi, T. 1989. Dynamic and static fusion gait of a quadruped walking vehicle. In *Proc. of IEEE/RSJ Int. Conf. on Intelligent Robots and Systems '89*, pp. 199–204.

Kimura, H., Shimoyama, I., and Miura, H. 1990. Dynamics in the dynamic walk of a quadruped robot. *RSJ. Advanced Robotics*, 4(3): 283–301.

Klein, C.A. and Chung, T.S. 1987. Force interaction and allocation for the legs of a walking vehcle. *Int. J. Robotics and Automation*, RA-3(6):546–555.

Klein, C.A. and Kittivatcharapong, S. 1990. Optimul force distribution for the legs of a walking machine with friction cone constraints. *Int. J. Robotics and Automation*, 6(1):73–85.

Lee, T. and Shih, C. 1988. A study of the gait control of a quadruped walking vehicle. *IEEE J. of Robotics and Automation*, 2(2):61–69.

Marhefka, D.W. and Orin, D.E. 1997. Gait planning for energy efficiency in walking machines. In *Proc. Int. Conf. on Robotics and Automation*, pp. 474–480.

Raibert, M.H. 1986. *Legged Robots That Balance*, MIT Press: Cambridge, MA.

Sano, A. and Furusho, J. 1989. Dynamically stable quadruped locomotion (a pace gait in the COLT-3). In *Proc. of the Int. Symp. on Industrial Robots*, pp. 253–260.

Yoneda, K. and Hirose, S. 1995. Dynamic and static fusion gait of a quadruped walking vehicle on a winding path. *Advanced Robotics*, 125–136.

Yoneda, K., Iiyama, H., and Hirose, S. 1986. Intermittent trot gait of a quadruped walking machine dynamic stability control of an omnidirectional walk. In *Proc. Int. Conf. on Robotics and Automation*, pp. 3002–3007.

Yoneda, K., Iiyama, H., and Hirose, S. 1994. Sky-hook suspention control of a quadruped walking vehicle. In *Proc. Int. Conf. on Robotics and Automation*, pp. 999–1004.

Ryo Kurazume is a researcher in Institute of Industrial Science at the University of Tokyo. He received his Ph.D. degree from the Department of Mechanical Engineering Science, Tokyo Institute of Technology in 1998. His M.E. and B.E. were from the Department of Mechanical Engineering Science, Tokyo Institute of Technology in 1991 and 1989, respectively. His research interests include multiple mobile robots, computer vision, and walking robots.

Kan Yoneda is an associate professor in the Department of Mechanical and Aerospace Engineering at Tokyo Institute of Technology. He received his Ph.D. degree from Department of Mechanical Engineering Science, Tokyo Institute of Technology in 1992. His M.S. and B.S. were from Department of Physics, Tokyo Institute of Technology in 1987 and 1985, respectively. His research interest includes mechanical design and control of biped, quadruped, and hexapod walking robot.

Shigeo Hirose was born in Tokyo, Japan in 1947. He is a Professor in the Department of Mechano-Aerospace Engineering at the Tokyo Institute of Technology. His research interests are in mechanisms, sensors and control of novel robotic systems. He was awarded more than twenty academic prizes including the Best Conference Paper Award in 1995 and the first Pioneer in Robotics and Automation Award in 1999 both from IEEE Robotics and Automation Society. He has published several books, including "Robotics" (Shokabo Publishing Co. Ltd., 1987, in Japanese) and "Biologically Inspired Robots" (Oxford University Press, 1993).